

# Occluded Iris Recognition using SURF Features

Anca Ignat<sup>1</sup> and Ioan Păvăloi<sup>2</sup>

<sup>1</sup>Faculty of Computer Science, University "Alexandru Ioan Cuza" of Iași, Romania

<sup>2</sup>Institute of Computer Science, Romanian Academy Iași Branch, Iași, Romania

**Keywords:** Iris Recognition, SURF, Occluded Iris Images, Manhattan Distance.

**Abstract:** In this paper we study the problem of the recognition process for iris images with missing information. Our approach uses keypoints related features for solving this problem. We present our recognition results obtained using SURF (Speeded-Up Robust Features) features extracted from occluded iris images. We tested the influence on the recognition rate of two threshold parameters, one linked with the SURF extraction process and the other with the keypoint matching scheme. The proposed method was tested on UPOL iris database using eleven levels of occlusion. The experiments show that the method we describe in this paper produces better results than Daugman procedure on all considered datasets and the results we previously obtained using SIFT features. Comparisons were also performed with iris recognition results that use colour for iris characterization, computed on the same databases of irises with different levels of missing information.

## 1 INTRODUCTION

There are many applications that use iris biometric features for automatic security and access control. This type of authentication that uses iris information is a non-invasive technology which provides a highly reliable solution. Generally, irises have a unique structure for each human being as those provided by fingerprints or the network of retinal blood vessels. For each person, the iris has a unique texture pattern that allows the process of person recognition. It's true that one major limitation is related to the image acquisition conditions, when images of the iris with occluded parts, or bad illumination can interfere with the recognition process. These types of problems require special approaches in order to have acceptable iris recognition results. One way to treat this problem is by using keypoint detectors that help extract the essential iris information.

Since the development of the famous Iris Code (Daugman, 1993, 2015), a lot of research was conducted on the problem of iris recognition. An excellent review of the methods and research directions in this field can be found in (Bowyer & Burge, 2016). De Marsico, Petrosino & Ricciardi, (2016) and Harakannavar & Puranikmath (2017) provide also excellent reviews on the iris recognition problem. In the pandemic context, when faces are covered by mask, the iris recognition problem becomes of increased interest. Nguyen et al. (2017)

present the research on long range iris recognition. Rattani & Derakhshani (2017) present a survey of methods that are analysing not only the iris but the entire region of the eye. A very interesting approach using deep learning tools are considered in Nguyen et al. (2017).

Considering the iris recognition problem with SURF descriptors, in (Ali et al., 2016) the effect of different enhancement methods as CLAHE, HE (Histogram Equalization), AHE (Adaptive Histogram Equalization) and classical matching procedure are tested. The method is tested on CASIA dataset and the results are compared with those obtained using SIFT, HOG, MSER and DAISY descriptors. The best results are in range 99.5% to 100% and are obtained with CLAHE. Mehrotra, Sa & Majhi (2013) propose a new iris segmentation procedure. The SURF features are extracted after segmentation. Image matching is performed using the Euclidean distance and the nearest neighbour ratio procedure. Experiments are conducted on different iris datasets: BATH, with the best results of 98.24%, UBIRIS, with 96.58%, and CASIA with 97.32%. The authors state that their method is robust to scale changes and rotations, occlusion and illumination changes. In the experiments performed on CASIA dataset by Bakshi et al. (2012), both SIFT and SURF features are extracted, the matching between two images being performed in three stages. After, the matching scores are combined.

Mehrotra, Majhi & Gupta (2009) apply SURF keypoint detection on the annular iris image. The usual normalization step is skipped to preserve as much iris information as possible. The matching procedure uses the Euclidean distance between the local features, two keypoints are paired if the distance between them is less than a fixed threshold. Three datasets are used in experiments, CASIA, BATH and IITD. In other experiments, Ismail, Ali & Farag (2015) before computing the SURF descriptors, CLAHE (Contrast Limited Adaptive Histogram Localization) enhancement technique is applied. The experiments are made on CASIA dataset. The matching procedure uses a fusion process of the scores obtained at different levels, the results range from 99.5% to 100%.

Păvăloi & Ignat (2018) introduce a new method for handling occluded iris images, using colour features. In Ignat & Vasiliu (2019) the problem of missing information is approached with an inpainting procedure. In Păvăloi & Ignat (2019b) SIFT descriptors are employed for solving the problem of iris recognition for irises with missing information.

We compute SURF descriptors in the present work and use them for iris recognition. For testing our method we used the original and the standardized segmented UPOL iris databases. For simulating the missing information situations, starting from UPOL dataset, we generated eleven datasets with different levels of occlusion. SURF feature extraction algorithm and the matching procedure depend on some threshold parameters. We tested the impact of these thresholds on the recognition results. We compare the results of our experiments with those obtained using Daugman procedure, implemented by Masek and with Păvăloi & Ignat (2019a, 2019b) results. We obtain better recognition rates on nine out of eleven datasets.

In Section 2 the datasets used in the experiments are presented. Section 3 outlines the SURF features extraction process and the recognition method. In section 4 are presented the results and the conclusions as well as future directions of research are stated in Section 5.

## 2 DATABASES

For our computations we used the well-known UPOL iris dataset (Dobeš et. Al, 2006, 2004). This dataset consists of iris images in .PNG format, all the images having the same dimensions  $576 \times 768 \times 3$  pixels (see the first image from Fig. 1). The collection contains iris images for 64 persons, six images for each individual, three for the right eye and three for the left

eye. The background of all these images is black. We first performed some experiments on the datasets that contain irises with full information. We have three versions for UPOL dataset, the original unsegmented, a manually segmented version (Păvăloi, Ciobanu & Luca, 2013) and a standardized segmented collection (Ignat, Luca & Ciobanu, 2016). In Fig. 1, a sample from each of these datasets are shown.

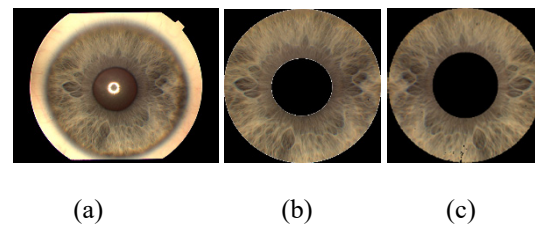


Figure 1: Examples of images in UPOL database: (a) - original, (b)- manually segmented, (c) – automatically segmented and standardized.

We performed some computations in order to decide which of the three versions of these datasets to further use in our experiments. The original, unsegmented dataset produced results that were inferior to those obtained on the other two datasets. The difference between the recognition rates obtained on the manually segmented dataset and the standardized one are almost the same (less than 1%).

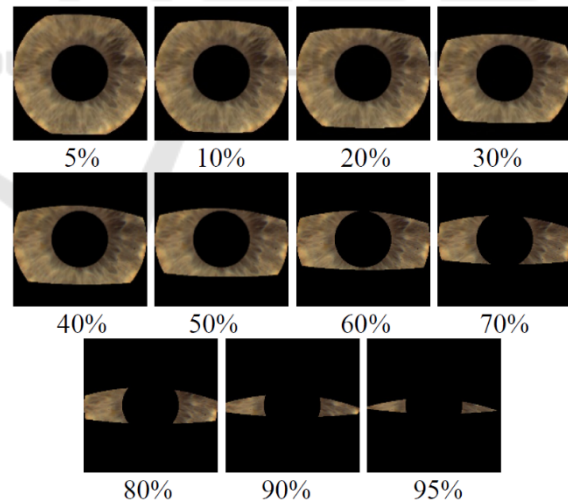


Figure 2: Samples from occluded UPOL datasets with missing information from 5%, 10% to 90%.

We decided to employ in our experiments the standardized UPOL dataset. The images in this dataset have  $404 \times 404 \times 3$  pixels, the region with iris information having the same size (the pupil zone has the same size). The eyelid-eyelash occlusion was simulated by cutting some regions from the lower and

upper part of the iris (see Fig 2). We eliminated more information from the upper part of the iris image than from the lower part. We eliminated iris information in such a way as to obtain images that have about 5%, 10%, 20%, 30%, 40%, 50%, 60%, 70%, 80%, 90% and 95% occlusion of the annular region of the iris.

### 3 SURF FEATURE EXTRACTION AND RECOGNITION METHOD

SURF, i.e. Speeded-Up Robust Features introduced in (Bay, Tuytelaars & Van Gool, 2006) is one of the most employed keypoints detector. As its name suggests, it is a faster and better version of SIFT descriptor. Around these keypoints, local features are extracted, having the same size, either 64 or 128 components. We chose for our experiments the variant with 128 elements. The number of keypoints that the SURF method computes, depends on the content of each image, two different images have different number of keypoints associated. For each one of these keypoints a feature vector with 128 components is calculated.

For the same image, one can compute different number of keypoints, depending on the choice of parameters involved in the SURF process, such as the threshold for the Hessian matrix or the number of the Gaussian pyramid octave or the number of octave layers within each octave.

We describe in the following the matching procedure between the keypoints of two images. The algorithm is an adaptation of the technique developed in (Păvăloi & Ignat, 2019). Assume we want to match two images,  $I$  and  $J$ . We first apply the SURF procedure to both of them. The SURF algorithm computes around the detected keypoints,  $m$  feature vectors,  $t_1, t_2, \dots, t_m$  for image  $I$  and  $n$  feature vectors  $d_1, d_2, \dots, d_n$  for image  $J$ .

Each image has a different number of feature vector associated ( $n \neq m$ ). We match keypoints from image  $I$  with keypoints from image  $J$  in the following way. We first compute all the distances from each feature vector associated with image  $I$  to all the feature vectors associated to image  $J$ .

The keypoint represented by feature vector  $t_i$  matches the keypoint represented by feature vector  $d_k$  if the following relation is fulfilled:

$$\text{dist}(t_i, d_k) \leq T \text{dist}(t_i, d_j), \quad j \neq k \quad (1)$$

where  $T > 0$  is a threshold parameter that allows to control the matching process. This type of matching is called nearest neighbor ratio matching procedure.

In equation (1) we tested three distances: Euclidean, Manhattan and Canberra.

After applying the SURF algorithm and performing the matching procedure, we define the distance between two images as the average of the distances between the coordinates of the matching keypoints.

$$d(I, J) = \text{average} \{ \| p_r - q_l \| \} \quad (2)$$

where  $p_r$  denote the coordinates of a keypoint from image  $I$  which is paired with a keypoint from image  $J$  with coordinates  $q_l$ . We used the Manhattan formula for computing the distances between the coordinates of the keypoints.

Denote by  $I$  the test image, and by  $S = \{J_p, p=1, s\}$  the training set. Assigning a label to image  $I$ , using the above described matching procedure is done by computing the following steps:

**Step 1:** Apply the SURF algorithm to  $I$  and all the images in  $S$ .

**Step 2:** Compute the number of matching points between the test image  $I$  and all the images from  $S$  using formula (1).

**Step 3:** Denote by  $m_p$  the number of matching points between the test image  $I$  and image  $J_p$ . Let  $q$  be the maximum number of matching points, i.e.

$$q = \max \{ m_p; p=1, \dots, s \} \quad (3)$$

Select from the training set a subset of images that have at least " $q-1$ " matching keypoints with the test image  $I$ .

**Step 4:** We compute the distances between test image  $I$  and the images selected after Step 3. Choose the image from the subset at minimum coordinates distance. The selected image will provide the label for the test iris image.

We tested the above mentioned three distances and the best results were obtained with Manhattan distance, so this is the distance that was used in our computations.

## 4 RESULTS

The number of extracted keypoints and feature vectors computed with SURF depends on the Hessian matrix threshold and the numbers of the pyramid octave. For this work we have tested how these parameters influence the recognition results. We experimentally found that the most important parameter, the parameter which made the difference, is the threshold for the Hessian blob detector in SURF features extraction method. We denote this threshold parameter by  $H$ . Our computations show that this

parameter is of most significance for the method we propose in this paper. Different values for this parameter produce sets of keypoints of different sizes. Smaller values for this threshold provide more detailed information about the analysed image, thus improving the iris recognition results. On the other hand, it is of interest to have as few SURF descriptors as possible, because this reduces the computation time in the matching process. In our computations we adopted a Leave-One-Out type of recognition method.

For each dataset, we have employed personalized values for the parameter  $H$ . We first computed some statistical values for each set of feature vectors, and different values of the threshold  $H$  parameter. These values are the total number of keypoints for the entire dataset, the minimum and maximum number of keypoints for the analysed images and the average number of keypoints. For this purpose, we used the segmented standardized UPOL dataset. The results are in Table 1.

Table 1: SURF statistics for the standardized segmented dataset.

Statistics/ $H \downarrow$	Total no	Min	Max	Average
100	195575	138	839	509.31
150	140669	81	705	366.33
200	106907	49	580	278.4
250	84644	26	484	220.43
300	68704	10	423	178.92
400	48492	4	321	126.28
500	36368	2	253	94.71

Obviously, small values for the  $H$  parameter produces large numbers of features and as its value increases the number of feature vectors decreases. We performed computations on both the original unsegmented UPOL dataset and for the standardized segmented dataset. For the first dataset the number of feature vectors was bigger than for the second one. For example, for  $H = 500$ , the original dataset has an average of 94840 features (and a recognition rate of 86.46%), and the standardized segmented dataset only 36368 features (recognition rate 94.71%). The reason why we use in our further computations the standardized segmented version of UPOL dataset is that we obtained better results on this dataset than on the other datasets.

It is obvious that the number of well recognized images increases when the number of extracted keypoints increases. One has to carefully choose the

$H$  parameter in order to balance the recognition results and the computing time.

Considering the following values for the threshold parameter involved in the matching process,  $T \in \{0.6, 0.7, 0.8\}$ , and for the Hessian related threshold  $H \in \{100, 200, 250, 300, 400, 500\}$  we obtain the recognition results depicted in Table 2.

Table 2: Number of well recognized images on standardized UPOL dataset.

T/H	100	200	250	300	400	500	Avg
0.6	382	378	372	369	358	342	366.83
0.7	384	378	373	371	364	350	370.00
0.8	381	375	369	363	347	335	361.67

Although the recognition results are very good, the processing time for  $H = 100$  is very big, because the number of detected keypoints is large, and each feature vector associated with these keypoints has to be compared with all the others. Anyway, for  $T = 0.7$  and  $H = 100$  the maximum number of recognized image (384) is achieved.

We also computed the number of well recognized images on the original UPOL dataset. The two threshold parameters that we analyse in this work were  $T \in \{0.5, 0.6, 0.7\}$ , and  $H \in \{200, 300, 400, 600, 1000\}$ , and the results are in Table 3. Note that the recognition results are lower than those computed for the segmented, standardized dataset. This emphasizes the fact that a good segmentation procedure yields good recognition results.

Table 3: Number of correctly recognized images on original UPOL.

T/H	200	300	400	600	1000	Avg
0.5	376	365	351	321	260	334.6
0.6	376	364	346	318	253	331.4
0.7	371	345	330	296	222	312.8

Considering the parameter  $H = 200$ , and computing the above mentioned statistics for the eleven datasets with different levels of missing iris information we get the results from Table 4.

From the statistics in this table we deduce that the number of feature vectors decreases as the level of iris occlusion increases. Starting with 60% missing information the average number of keypoints is less than 200 and for 90% and for 95% missing information the average is less than 100. Sure, one can force SURF to compute more features by choosing smaller values for the  $H$  threshold parameter, but this comes with the inconvenience of a very long computing time.

Table 4: SURF statistics for occluded datasets H= 200, T= 0.7.

Statistics/ Occlusion	Total no	Min	Max	Average
05	11095	54	5	288.95
10	11090	57	571	288.81
20	10579	54	541	275.51
30	98312	45	508	256
40	91958	245	458	239.4
50	84561	33	433	220.2
60	73765	29	365	192.1
70	55860	28	284	145.4
80	43606	15	218	113.56
90	3220	15	149	83.87
95	2413	15	117	62.85

In Table 5 we present the number of correctly classified images for H=200, T=0.7 for irises with occlusions. We performed computations on the entire dataset and separately on the left eye and on the right eye.

Note that the results are very good (98.95% for 70% missing information). For images with 10% or 5% iris information the SURF descriptor is unable to compute sufficient keypoints to have good recognition results. Note that, on average, the recognition results are similar for the complete dataset, right eye and left eye (95.45% for both eye dataset, 95.97% for the left eye, and 96.07% for the right eye). An interesting situation occurs for the left eye dataset with 70% missing information, in this case the recognition rate is 100%.

Table 5: Recognition results for dataset with occlusion, H= 200, T= 0.7.

Recogn. / Occlusion	Left+Right eye	Left eye	Right eye
05	382	192	190
10	381	191	191
20	382	190	192
30	381	192	190
40	380	192	189
50	383	192	191
60	379	190	191
70	380	192	190
80	378	190	188
90	339	168	175
95	267	138	142

In the sequel, we focused our attention on the two datasets with the smallest amount of iris information. For  $H \in \{25, 50, 100, 150\}$  our method applied on the

datasets with 90% and 95% of missing information will produce the results Table 6.

Table 6: SURF statistics for occluded datasets with 90% and 95% occlusion, T=0.7.

	Total no	Min	Max	Avg.
90% H=50	66871	89	230	174.14
90% H=100	48468	36	194	126.22
90% H=150	39035	20	170	101.65
95% H=25	57093	96	183	148.68
95% H=50	50753	59	176	132.17
95% H=100	36891	25	155	96.07
95% H=150	29459	17	136	76.74

The recognition results in terms of correctly classified images, for the datasets and parameters used in Table 6 are in Table 7. For the complete dataset with 90% missing information one gets a very good recognition rate of 95.31%, for T=0.7, and H=50. For the complete dataset with only 5% of iris information, the best recognition result (89.58%) is obtained for T=0.7 and H=25. For the right eye dataset with 95% missing information and H=25 we get an excellent 95.31% recognition result. We remarked that, in this situation, the right eye dataset has a better average recognition rate (90.25%) than the complete dataset (86.97%) and the left eye (87.27%).

Table 7: Recognition results for occluded datasets with 90% and 95% missing information, T=0.7.

	Left+Right eye	Left eye	Right eye
90% H=50	366	180	187
90% H=100	356	176	181
90% H=150	348	177	178
95% H=25	344	170	183
95% H=50	335	169	173
95% H=100	303	154	157
95% H=150	286	147	154

In Table 8 we compare the results obtained with this method, those obtained in Pāvāloi & Ignat (2019a,2019b) in two papers from 2019, one using only SIFT features, and the other using colour and SIFT features. We also compare our results with Daugman's Iris Code (Daugman, 1993, 2015), algorithm that was implemented by Masek (Masek, 2003).

Table 8: Comparison results with other methods for the segmented standardized UPOL dataset,  $T=0.7$

Methods/ Miss. Info.	(PI,a)	(PI,b)	Daugmann- Masek	Our method
0	<b>384</b>	374	382	<b>384</b>
05	382	372	381	<b>382</b>
10	380	374	380	<b>381</b>
20	377	376	378	<b>382</b>
30	<b>382</b>	378	377	381
40	<b>380</b>	377	377	<b>380</b>
50	381	374	375	<b>383</b>
60	377	374	370	<b>379</b>
70	375	373	361	<b>380</b>
80	369	375	341	<b>378</b>
90	305	<b>369</b>	316	366
95	174	<b>367</b>	275	344

In the last column of Table 8 the results were obtained with different values for the blob detection related threshold,  $H$  (the values that provided the best results). We get better recognition results in nine out of the twelve analysed experiments. For the cases of 90% and 95% missing information the SURF procedure extracts very few keypoints and thus the recognition rate is lower. The method that provides better results in these situations, although uses a keypoint detector, but the results are improved in these case, by the colour features (Pāvāloi & Ignat, 2016).

The images from the standardized UPOL collection are very regular, the annular iris region and the pupil have the same size in all the images. We tested our method on images with an irregular structure of the iris, and non-uniform background, by performing some computations on the images from the original UPOL collection. We considered three cases, namely images with 30%, 60% and 90% missing information (see Fig. 3).

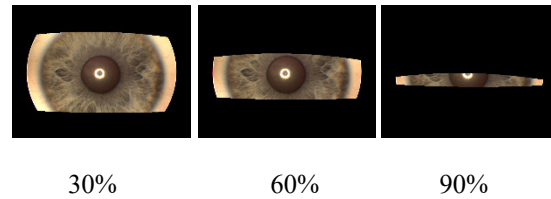


Figure 3: Examples of iris images with missing information from the original UPOL database: 30%, 60%, 90%.

We used, as before,  $H=200$  and  $T=0.7$ . The results of our computations are in Table 9. In this case, due to the fact that the image contains non-iris information, the recognition rate decreases more rapidly as the occlusion increases.

Table 9: Recognition results for the original UPOL dataset, 30%, 60%, 90% missing information.

Missing info.	Left+Right eye	Left eye	Right eye
0	371	186	186
30	354	180	175
60	342	168	176
90	245	126	119

We analyzed the importance of a standard iris segmentation by applying our method on the manually segmented UPOL. The iris images in this dataset have variable iris and pupil areas (see Fig. 4). The background is black. We used the same values of the threshold parameters,  $H=200$  and  $T=0.7$ . The results are in Table 10. Note that in this case the results are lower than those obtained for the other two datasets. One reason for these results is the fact that SURF extracts orientation and shape information around the keypoints. Another reason for these differences is the distance (2) we use in the classification process. For very regular images, such as the images from the standardized UPOL collection, this distance works. For the other datasets one needs to find a new distance. A third reason is the fact that the  $H$  parameter need to be carefully chosen for each dataset in order to obtain good recognition results.

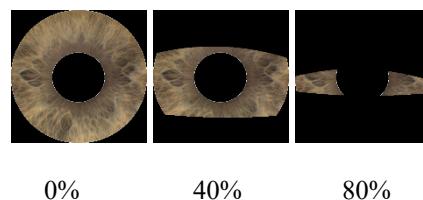


Figure 3: Examples of iris images with missing information from the manually segmented UPOL database: 0%, 40%, 80%.

Table 10: Recognition results for the manually segmented UPOL dataset, 10% to 90% missing information.

Missing info.	Left+Right eye	Left eye	Right eye
10	346	178	182
20	342	176	179
30	339	178	176
40	329	175	170
50	322	168	168
60	321	164	168
70	290	160	153
80	259	138	135
90	178	93	106

One way to improve the results for datasets with irregular shape of the iris images is to add texture information to the feature vectors extracted around the keypoints.

## 5 CONCLUSIONS

This paper presents the computation results on occluded iris image recognition using SURF features and an adapted method we previously developed for SIFT keypoint detection. In experiments, the UPOL iris dataset was employed. We obtain, in some situations, better results than those computed with SIFT based features. We observed that the recognition accuracy depends on the number SURF features but after a certain level, the recognition rate reaches a plateau. For each dataset, the value of the Hessian threshold parameter used for computing SURF features must be established after some experiments. Usually, an average bigger than 200 SURF descriptors for an image seems to give very good recognition results. Sure, for datasets with 90% or 95% missing information that target cannot be reached. Experiments have revealed that a good value for the matching threshold parameter is 0.7.

In our future work we intend to employ also other datasets, as UBIRIS for example. In our future experiments we are interested in combining SURF method with texture features and the colour information.

## REFERENCES

- Daugman, J. G. (1993). High confidence visual recognition of persons by a test of statistical independence. *IEEE transactions on pattern analysis and machine intelligence*, 15(11), 1148-1161.
- Daugman, J. (2015). Information theory and the iriscodes. *IEEE transactions on information forensics and security*, 11(2), 400-409.
- Bowyer, K. W., & Burge, M. J. (Eds.). (2016). *Handbook of iris recognition*. Springer London.
- De Marsico, M., Petrosino, A., & Ricciardi, S. (2016). Iris recognition through machine learning techniques: A survey. *Pattern Recognition Letters*, 82, 106-115.
- Harakannavar, S. S., & Puranikmath, V. I. (2017, December). Comparative survey of iris recognition. In *2017 International Conference on Electrical, Electronics, Communication, Computer, and Optimization Techniques (ICEECCOT)* (pp. 280-283). IEEE.
- Nguyen, K., Fookes, C., Jillela, R., Sridharan, S., & Ross, A. (2017). Long range iris recognition: A survey. *Pattern Recognition*, 72, 123-143.
- Rattani, A., & Derakhshani, R. (2017). Ocular biometrics in the visible spectrum: A survey. *Image and Vision Computing*, 59, 1-16.
- Nguyen, K., Fookes, C., Ross, A. & Sridharan, S. (2017) Iris recognition with off-the-shelf CNN features: A deep learning perspective. *IEEE Access*, 6, 18848-18855.
- Ali, H. S., Ismail, A. I., Farag, F. A., & Abd El-Samie, F. E. (2016). Speeded up robust features for efficient iris recognition. *Signal, Image and Video Processing*, 10(8), 1385-1391.
- Mehrotra, H., Sa, P. K., & Majhi, B. (2013). Fast segmentation and adaptive SURF descriptor for iris recognition. *Mathematical and Computer Modelling*, 58(1-2), 132-146.
- Bakshi, S., Das, S., Mehrotra, H., & Sa, P. K. (2012, March). Score level fusion of SIFT and SURF for iris. In *2012 International Conference on Devices, Circuits and Systems (ICDCS)* (pp. 527-531). IEEE.
- Mehrotra, H., Majhi, B., & Gupta, P. (2009, December). Annular iris recognition using SURF. In *International Conference on Pattern Recognition and Machine Intelligence* (pp. 464-469). Springer, Berlin, Heidelberg.
- Ismail, A. I., Ali, H. S., & Farag, F. A. (2015, February). Efficient enhancement and matching for iris recognition using SURF. In *2015 5th national symposium on information technology: Towards new smart world (NSITNSW)* (pp. 1-5). IEEE.
- Pāvāloi, I., & Ignat, A. (2018, September). Experiments on Iris Recognition Using Partially Occluded Images. In *International Workshop Soft Computing Applications* (pp. 153-173). Springer, Cham.
- Ignat, A., & Vasiliu, A. (2018). A study of some fast inpainting methods with application to iris reconstruction. *Procedia Computer Science*, 126, 616-625.
- Pāvāloi, I., & Ignat, A. (2019). Iris Image Classification Using SIFT Features. *Procedia Computer Science*, 159, 241-250.

- Dobeš, M., Martinek, J., Skoupil, D., Dobešová, Z., & Pospíšil, J. (2006). Human eye localization using the modified Hough transform. *Optik*, 117(10), 468-473.
- Dobeš, M., Machala, L., Tichavský, P., & Pospíšil, J. (2004). Human eye iris recognition using the mutual information. *Optik*, 115(9), 399-404.
- Păvăloi, I., Ciobanu, A., & Luca, M. (2013, November). Iris classification using WinICC and LAB color features. In *2013 E-Health and Bioengineering Conference (EHB)* (pp. 1-4). IEEE.
- Ignat, A., Luca, M., & Ciobanu, A. (2016). New Method of Iris Recognition Using Dual Tree Complex Wavelet Transform. In *Soft Computing Applications* (pp. 851-862). Springer, Cham.
- Bay, H., Tuytelaars, T., & Van Gool, L. (2006, May). Surf: Speeded up robust features. In *European conference on computer vision* (pp. 404-417). Springer, Berlin, Heidelberg.
- Păvăloi, I., & Ignat, A. (2019, November). Iris Occluded Image Classification Using Color and SIFT Features. In *2019 E-Health and Bioengineering Conference (EHB)* (pp. 1-4). IEEE.
- Masek, L. (2003). *Recognition of human iris patterns for biometric identification* (Doctoral dissertation, Master's thesis, University of Western Australia).
- Masek, L. (2003). Matlab source code for a biometric identification system based on iris patterns. <http://people.csse.uwa.edu.au/pk/studentprojects/libor/>.
- Păvăloi, I., & Ignat, A. (2016, August). Iris recognition using color and texture features. In *International workshop soft computing applications* (pp. 483-497). Springer, Cham.

